

Capture of α Particles by Isospin-Symmetric Nuclei

T. Rauscher, F.-K. Thielemann

Departement für Physik und Astronomie, Universität Basel, CH-4056 Basel, Switzerland

J. Görres, M. Wiescher

Department of Physics, University of Notre Dame, Notre Dame, IN 46556, USA

Abstract

The reaction rates for α capture processes on self-conjugate nuclei in the mass range $A=20-40$ have been investigated. The rates were calculated using the statistical model code NON-SMOKER taking into account isospin suppression rules. These theoretical predictions are compared with rates derived from the available experimental data about the α capture reactions taking also into account additional experimental information from different reaction channels populating the α unbound states of the self-conjugate compound nuclei.

I. INTRODUCTION

The astrophysical importance of α capture on target nuclei with $N = Z$ is manifold. In the Ne- and O-burning phase of massive stars, alpha capture reaction sequences are initiated at ^{24}Mg and ^{28}Si , respectively, and determine the abundance distribution prior to the Si-burning phase [1]. Nucleosynthesis in explosive Ne and explosive O burning in type II supernovae depend on reaction rates for α capture on ^{20}Ne to ^{36}Ar [2,3]. While many of these processes are in quasistatistical equilibrium [3–5], the reaction rates itself are important for a reliable description of nucleosynthesis in the subsequent cooling phase. An α capture chain on such self-conjugate nuclei actually determines the production of ^{44}Ti [6], which contributes to the light curve by its β decay to ^{44}Ca via ^{44}Sc . Charged-particle reaction networks have to consider α -rates in the conditions of an α -rich freeze-out [7], or an extended rp-process [8,9]. Such calculations involve also highly unstable nuclei, thus calling for a reliable prediction of the respective reaction rates.

Due to isospin selection rules, $E1\gamma$ transitions with isospin $T = 0 \rightarrow T = 0$ are forbidden. Likewise, $M1$ transitions will be strongly suppressed. Because of isospin conservation, only states with isospin $T = 0$ can be populated by α capture on $N = Z$ ($T = 0$) targets. This leads to a strong suppression of the γ transitions in the compound nucleus and thus of the (α, γ) cross section of self-conjugate nuclei [10].

Previous theoretical work used in astrophysical calculations either neglected this isospin effect [11,12] or accounted for it only in a phenomenological way with arbitrary suppression factors [13–15,9]. In this work we want to improve on the prediction of reaction rates on isospin-symmetric targets and compare the theoretical values to newly compiled available experimental information. In section II the statistical model of nuclear reactions is

introduced and the method for obtaining isospin suppression factors as well as the resulting theoretical cross sections and reaction rates are presented. Section III reviews the available experimental information and presents reaction rates newly derived from all available experimental data covering different reaction channels. A summary and conclusion will be given in Section IV.

II. THE STATISTICAL MODEL

A. Introduction

The majority of nuclear reactions in astrophysics can be described in the framework of the statistical model (compound nucleus mechanism, Hauser-Feshbach approach, HF; see e.g. [16,17]), provided that the level density of the compound nucleus is sufficiently large in the contributing energy window [19]. This description assumes that the reaction proceeds via a compound nucleus which finally decays into the reaction products. With a sufficiently high level density, average cross sections

$$\sigma^{\text{HF}} = \sigma_{\text{form}} b_{\text{dec}} = \sigma_{\text{form}} \frac{\Gamma_{\text{final}}}{\Gamma_{\text{tot}}} \quad (1)$$

can be calculated which can be factorized into a cross section σ_{form} for the formation of the compound nucleus and a branching ratio b_{dec} , describing the probability of the decay into the channel of interest compared with the total decay probability into all possible exit channels. The partial widths Γ as well as σ_{form} are related to (averaged) transmission coefficients, which comprise the central quantities in any HF calculation.

Many nuclear properties enter the computation of the transmission coefficients: mass differences (separation energies), optical potentials, GDR widths, level densities. The transmission coefficients can be modified due to pre-equilibrium effects which are included in width fluctuation corrections [18] (see also [19], and references therein) and by isospin effects. It is in the description of the nuclear properties where the various HF models differ.

In astrophysical applications usually different aspects are emphasized than in pure nuclear physics investigations. Many of the latter in this long and well established field were focused on specific reactions, where all or most "ingredients", like optical potentials for particle transmission coefficients, level densities, resonance energies and widths of giant resonances to be implemented in predicting E1 and M1 γ -transitions, were deduced from experiments. As long as the statistical model prerequisites are met, this will produce highly accurate cross sections. For the majority of nuclei in astrophysical applications such information is not available. The real challenge is thus not the well-established statistical model, but rather to provide all these necessary ingredients in as reliable a way as possible, also for nuclei where none of such information is available.

B. The NON-SMOKER Code

For the calculations presented in this work we utilized the recently developed statistical model code NON-SMOKER [20]. The current status of the code is outlined in the following.

For neutrons and protons the optical potential of Jeukenne, Lejeune & Mahaux (1977) [21] is used, which is based on microscopic infinite nuclear matter calculations for a given density, applied with a local density approximation. It includes corrections of the imaginary part [24,22]. The potential of McFadden & Satchler (1966) [23] is used for α particles, which is based on extensive data. Deformed nuclei are treated by an effective spherical potential of equal volume (see e.g. [12,15]).

The level density treatment has been recently improved [19]. Additionally, experimental level information (excitation energies, spins, parities) are included [25], as well as experimental nuclear masses [26].

The γ -transmission coefficients have to include the dominant E1 and M1 γ transitions. The smaller, less important M1 transitions have usually been treated with the simple single particle approach $T \propto E^3$ (see e.g. [27]). The E1 transitions are usually calculated on the basis of the Lorentzian representation of the Giant Dipole Resonance (GDR). Many microscopic and macroscopic models have been devoted to the calculation of GDR energies and widths. An excellent fit to the GDR energies is obtained with the hydrodynamic droplet model [28]. An improved microscopic-macroscopic approach is used, based on dissipation and the coupling to quadrupole surface vibrations [29]; see also [15]. Most recently it was shown [30] that the inclusion of “soft mode” or “pygmy” resonances might have important consequences on the E1 transitions in neutron-rich nuclei far off stability. The pygmy resonances could be caused by a neutron skin which generates soft vibrational modes [31]. It is still under discussion whether such modes exist. As the effect is negligible for nuclei close to stability, we did not include it in the calculations presented here.

C. Inclusion of Isospin Effects

The original Hauser-Feshbach equation [16] implicitly assumes complete isospin mixing but can be generalized to explicitly treat the contributions of the dense background states with isospin $T^< = T^{\text{g.s.}}$ and the isobaric analog states with $T^> = T^< + 1$ [32,17,33,34]. In reality, compound nucleus states do not have unique isospin and for that reason an isospin mixing parameter $\mu \downarrow$ was introduced [32], which is the fraction of the width of $T^>$ states leading to $T^<$ transitions; for complete isospin mixing $\mu \downarrow = 1$, for pure $T^<$ states $\mu \downarrow = 0$. In the case of overlapping resonances for each involved isospin, $\mu \downarrow$ is directly related to the level densities $\rho^<$ and $\rho^>$, respectively. Isolated resonances can also be included via their internal spreading width Γ^{\downarrow} and a bridging formula was derived to cover both regimes [35].

In order to determine the mixing parameter $\mu \downarrow = \mu \downarrow(E)$, experimental information for excitation energies of $T^>$ levels is used where available [25,36] in the code NON-SMOKER. Experimental values for spreading widths are also tabulated [34,36]. Similarly to the standard treatment for the $T^<$ states, a level density description [19] is invoked above the last experimentally known $T^>$ level. Since the $T^>$ states in a nucleus (Z, N) are part of a multiplet, they can be approximated by the levels (and level density) of the nucleus $(Z-1, N+1)$, only shifted by a certain energy E_d . This displacement energy E_d can be calculated [37] and it is dominated by the Coulomb displacement energy: $E_d = E_d^{\text{Coul}} + \epsilon$. In the absence of experimental level information, we use the formula from Woosley & Fowler as given by [38] for the determination of the excitation energy of the first isobaric analog state.

The inclusion of the explicit treatment of isospin has two major effects on statistical cross section calculations in astrophysics: the suppression of γ widths for reactions involving self-conjugate nuclei and the suppression of the neutron emission in proton-induced reactions. This paper focuses on the suppression of the γ width in α capture reactions. Non-statistical effects, i.e. the appearance of isobaric analog resonances, will not be further discussed here.

The isospin selection rule for $E1$ transitions is $\Delta T = 0, 1$ with transitions $0 \rightarrow 0$ being forbidden. In the case of (α, γ) reactions on targets with $N = Z$, the cross sections will be heavily suppressed because $T = 1$ states cannot be populated in the compound nucleus due to isospin conservation. A suppression will also be found for capture reactions leading into self-conjugate nuclei, although somewhat less pronounced because $T = 1$ states can be populated according to the isospin coupling coefficients.

In previous reaction rate calculations [13–15,9] the suppression of the γ widths was treated completely phenomenologically by dividing the *total* γ widths (and thus the cross section) by quite uncertain factors of 5 and 2, for (α, γ) reactions on self-conjugate nuclei and nucleon capture reactions going into self-conjugate nuclei, respectively, regardless of the target’s nature. These empirical factors were estimated from the scarce experimental data [39] available at that time.

We are replacing these factors by including more isospin information into the calculation of the $E1$ and $M1$ suppression. It can be shown (see e.g. [40]) that $0 \rightarrow 0$ $E1$ transitions are forbidden. An approximate suppression rule for $\Delta T = 0$ transitions in self-conjugate nuclei can also be derived for $M1$ transitions [40] and leads to a suppression factor of about 1/150. The total suppression of the $E1$ transitions would be exact if isospin were an exact quantum number, at least in the simplifying limit that the wavelength of the transition involved is large compared with the nuclear size. However, the Coulomb force mixes states of different isospin to a small extent, so the “clean” selection rule becomes a suppression factor, too. The theoretical estimate for the factor as given by Ref. [40] is 0.01.

Since only $T^< = 0$ states can be populated by α capture, we need to know the mixing of these $T^<$ into $T^>$ states. Below the first isobaric analog state at E_d , states should be unmixed. We describe that phenomenologically by suppressing both $E1$ and $M1$ transitions. The suppression factor f_{iso} is set equal for $E1$ and $M1$.

It is clear that the total suppression factor of the resulting γ width must be related to the number of resonances in the compound nucleus. Therefore, in a straightforward way we set the suppression for γ transitions from the excitation energy E of the compound nucleus proportional to the ratio of the density of $T = 1$ levels and the density of $T = 0$ levels,

$$f_{\text{iso}}(E) \propto \frac{\rho^>(E)}{\rho^<(E)} . \quad (2)$$

We find a weak energy dependence of f_{iso} .

D. Results

The cross sections and reaction rates for α capture were calculated for the $N = Z$ isotopes from Mg to Mo ($12 \leq Z \leq 42$). The NON-SMOKER results including the above description of isospin suppression of the γ width are given in Tables VII to XII. In the next section we

compare these results to experimental cross sections and rates, either directly measured or calculated from resonance parameters.

III. COMPARISON TO EXPERIMENTAL INFORMATION

A. Experimental data

Experimental data on α capture reactions on self-conjugate nuclei $20 \leq A \leq 40$ are rather sparse. To determine reliably the reaction rate at various stellar temperatures T_9 (in GK) detailed information on the number of contributing resonances n , the resonance strengths $\omega\gamma_i$ (in units eV), and the resonance energies E_i (in units MeV) are necessary:

$$N_A \langle \sigma v \rangle = 1.54 \cdot 10^5 \cdot A^{-3/2} T_9^{-3/2} \cdot \sum_i^n \omega\gamma_i \cdot e^{\frac{-11.605 \cdot E_i}{T_9}} , \quad (3)$$

with A as the reduced mass of the system. The resonance strength depends on the spin of the resonance J and the partial widths of the entrance Γ_α and exit channel Γ_γ , and the total width Γ

$$\omega\gamma = 2J + 1 \cdot \frac{\Gamma_\alpha \cdot \Gamma_\gamma}{\Gamma} . \quad (4)$$

Extensive resonance studies in the astrophysically relevant low energy range $E_\alpha \leq 1.5$ MeV have only been made for $^{20}\text{Ne}(\alpha, \gamma)^{24}\text{Mg}$ [41], $^{24}\text{Mg}(\alpha, \gamma)^{28}\text{Si}$ [43,42], and also for $^{28}\text{Si}(\alpha, \gamma)^{32}\text{S}$ [44]; [45]. For the reaction $^{32}\text{S}(\alpha, \gamma)^{36}\text{Ar}$ only insufficient data are available on resonances in the energy range $E_\alpha \geq 2.2$ MeV [46–48]. The experimentally observed level density in the compound nucleus ^{36}Ar indicates a significantly higher number of possible resonances [49]. Even less information is available on resonances in $^{36}\text{Ar}(\alpha, \gamma)^{40}\text{Ca}$. Resonance measurements have been performed in the energy range of the giant dipole resonance $E_\alpha = 6$ –17 MeV. Several strong resonances have been observed and the resonance strengths were determined [50]. Measurements at lower energies, however, $E_\alpha = 3$ –6 MeV, did not yield any significant information on possible resonance states in this range [51]. More experimental data are again available for the reaction $^{40}\text{Ca}(\alpha, \gamma)^{44}\text{Ti}$. Several resonances were successfully measured in the energy range $E_\alpha = 2.75$ –4 MeV [39], additional measurements were performed in the energy range $E_\alpha = 4$ –6 MeV [52,53]. Again, no information is available on lower energy resonances.

Due to the lack of low energy resonance information a direct comparison of the predicted HF rates and the rates obtained by the experimental data is only of limited use. However, additional and complementary information can be gained from resonance α elastic scattering measurements and lifetime measurements which yield information about the total width Γ of the resonance state. More important, however, are (p, α) studies with a self-conjugate compound nucleus. These measurements yield extensive information about the existence and characteristics of possible resonances in the α capture channel. In particular reactions like $^{23}\text{Na}(p, \alpha)^{20}\text{Ne}$ [49,54], $^{27}\text{Al}(p, \alpha)^{24}\text{Mg}$ [49], $^{31}\text{P}(p, \alpha)^{28}\text{Si}$ [55–57] $^{35}\text{Cl}(p, \alpha)^{32}\text{S}$ [58,57], and $^{39}\text{K}(p, \alpha)^{36}\text{Ar}$ populate α -unbound natural parity states in the self-conjugate compound nuclei and therefore complement the direct experimental information on resonances

in $^{20}\text{Ne}(\alpha, \gamma)^{24}\text{Mg}$, $^{24}\text{Mg}(\alpha, \gamma)^{28}\text{Si}$, $^{28}\text{Si}(\alpha, \gamma)^{32}\text{S}$, $^{32}\text{S}(\alpha, \gamma)^{36}\text{Ar}$, and $^{36}\text{Ar}(\alpha, \gamma)^{40}\text{Ca}$, respectively. Particularly useful is information on the resonance strength,

$$\omega_{\gamma(p,\alpha)} = \frac{2J+1}{(2j_p+1)(2j_t+1)} \cdot \frac{\Gamma_p \cdot \Gamma_\alpha}{\Gamma} \quad (5)$$

with j_p and j_t as projectile and target spin. Combined with information on the total width

$$\Gamma \approx \Gamma_p + \Gamma_\alpha \quad (6)$$

and on the resonance strengths of the correlated natural parity (p, γ) resonances

$$\omega_{\gamma(p,\gamma)} = \frac{2J+1}{(2j_p+1)(2j_t+1)} \cdot \frac{\Gamma_p \cdot \Gamma_\gamma}{\Gamma}. \quad (7)$$

Such information allows to fit the partial widths Γ_p , Γ_γ , Γ_α to match the total width and the observed (p, γ) and (p, α) strengths. The (α, γ) resonance strength is calculated from these values. If only partial data about (p, γ) or (p, α) resonance strengths and the total width is available, we adopted an alpha spectroscopic factor from empirical alpha-strength studies in self-conjugate nuclei in this mass range [59] and calculated the α width of the level in terms of a simple potential model. If only either the total width, or one of the (p, γ) or (p, α) strengths is available, both the alpha as well as the proton partial width need to be calculated. For the latter case the single particle spectroscopic factor was adopted from the average of the single particle strength distribution in the excitation range of this nucleus. For natural parity levels with no spectroscopic information available, the gamma width was calculated additionally. We used an average Weisskopf strength which has been matched to the known gamma strength distribution of the neighboring states to account empirically for the isospin γ strength suppression in self-conjugate nuclei. Since there are no data available for proton capture on the short-lived ^{43}Sc , the strengths of low energy resonances in $^{40}\text{Ca}(\alpha, \gamma)^{44}\text{Ti}$ are based purely on such estimates. The results are listed and compared with the available experimental data in Table I to VI. It can clearly be seen that there is systematically good agreement between the calculated and experimental resonance parameters.

B. Reaction Rates

The resonance parameters derived and discussed in the previous chapter allow us to calculate the reaction rate $N_A \langle \sigma v \rangle$ as a function of temperature using Equation 2. These rates are directly compared with the reaction rates $N_A \langle \sigma v \rangle_{\text{HF}}$ based on the HF calculations with the code NON-SMOKER in Tables VII to XII. Shown is the 'experimental' reaction rate $N_A \langle \sigma v \rangle_{\text{exp}}$ which is based on the few directly observed (α, γ) resonances only. The 'empirical' rate $N_A \langle \sigma v \rangle_{\text{emp}}$ is calculated using Equation 2 on the basis of the extended resonance set and the associated level parameter analysis discussed in the previous section. The ratios of the 'experimental' to the 'empirical' rates is shown in Figs. 1–6. For the reactions $^{20}\text{Ne}(\alpha, \gamma)^{24}\text{Mg}$, $^{24}\text{Mg}(\alpha, \gamma)^{28}\text{Si}$, and $^{28}\text{Si}(\alpha, \gamma)^{21}\text{S}$ a considerable amount of experimental alpha capture data is available for higher energies [41,42,44,45], therefore at temperatures above $T \approx 0.3$ GK the experimental rates are in good agreement with the

empirical rates, only at lower temperatures the experimental rates are substantially lower due to the lack of experimental data. Only very limited data on alpha capture resonances are available for $^{32}\text{S}(\alpha, \gamma)^{36}\text{Ar}$ and $^{36}\text{Ar}(\alpha, \gamma)^{40}\text{Ca}$, this explains the substantial deviation between experimental and empirical rate over the entire temperature range.

The ratios of the statistical model rates discussed in Section II and empirical rates discussed in Section III are shown in Fig. 7 for the astrophysically relevant temperature region. Except for $^{40}\text{Ca}(\alpha, \gamma)^{44}\text{Ti}$, the deviations remain in the range of a factor of ≤ 3 . This is to be expected from a global statistical model calculation. Towards higher temperature ($T \geq 3.5$ GK) the calculation is significantly improved in respect to the empirical rate and reaches a deviation of about 30%.

Towards lower temperature two different behaviors can be identified. The ratios of $^{20}\text{Ne}(\alpha, \gamma)^{24}\text{Mg}$ and $^{40}\text{Ca}(\alpha, \gamma)^{44}\text{Ti}$ increase towards lower temperatures, whereas the other ratios first decrease and finally strongly increase at the lowest temperatures $T \leq 0.2$ GK (not shown in Fig. 7 as the corresponding rates are already very low and outside the temperature region of interest). In the latter very low temperature range the reaction rates are dominated by low energy resonances, $E_R \leq 1$ MeV. For these resonances the α width Γ_α is typically smaller than the γ width and determines the resonance strength $\omega\gamma_{(\alpha,\gamma)}$. The reduction of γ -strength has no influence for these states. With only a few dominating resonances the assumptions of the statistical model are not valid anymore.

For the decrease of the ratios in the temperature range $T < 3$ GK the proper energy dependence of the optical α +nucleus potential is an important factor. The slope of the ratio plotted in Fig. 7 for each reaction is sensitive to the choice of the optical potential. The use of an equivalent square well potential which neglects absorption in the Coulomb barrier leads to a slightly less steep slope. Apparently, all available α +nucleus potentials in statistical model calculations cannot account for the proper energy dependence at energies close to the Coulomb barrier. This is a well-known problem in such calculations.

The cases for $^{20}\text{Ne}(\alpha, \gamma)^{24}\text{Mg}$ and $^{40}\text{Ca}(\alpha, \gamma)^{44}\text{Ti}$ seem different, there the HF predictions are larger than the empirical rate and the ratios increase monotonically towards lower temperatures. However, the HF calculation is in agreement within a factor of about 2 for the temperature range $T \geq 0.4$ GK with the experimental value directly derived from α capture resonances in the reaction $^{20}\text{Ne}(\alpha, \gamma)$. For $^{40}\text{Ca}(\alpha, \gamma)$, the empirical rate is nearly identical with the experimental rate for temperatures $T = 1 - 5$ GK as can be seen from figure 6. Most of the available experimental information about natural parity states in ^{44}Ti is based on α capture studies [39,52,53]. Only two α unbound states at lower energies, $E_x \leq 7.5$ MeV, are known from $^{46}\text{Ti}(\text{p},\text{t})^{44}\text{Ti}$ two-particle transfer measurements [49]. Also the results of $^{40}\text{Ca}(\text{Li},\text{d})^{44}\text{Ti}$ and $^{40}\text{Ca}(\text{Li},\text{t})^{44}\text{Ti}$ α -transfer measurements [60,61] indicate a fairly low level density in the excitation range of interest. Shell model calculations support the experimental results that the level density in the pf-shell nucleus ^{44}Ti is low [62]. The low level density in ^{44}Ti may limit the applicability of the HF approach for calculating the reaction rate of $^{40}\text{Ca}(\alpha, \gamma)^{44}\text{Ti}$. This is supported by the fact that a variation in the level density description employed in the statistical model calculation has a significant impact on the reaction rate of $^{40}\text{Ca}(\alpha, \gamma)^{44}\text{Ti}$ but leaves the remaining rates nearly unchanged. This high sensitivity is due to the low level density in the compound nucleus.

IV. SUMMARY AND CONCLUSION

In this paper we attempted to improve the statistical model description of α capture rates on self-conjugate nuclei, which are important for many nucleosynthesis processes in stellar and explosive He-burning.

The NON-SMOKER predictions presented here are typically lower than the results of previous Hauser-Feshbach calculations [13,14], except for $^{28}\text{Si}(\alpha,\gamma)^{32}\text{S}$ for which the present theoretical rate is higher by a factor of 1.96 (see also Table 6 in [6]). Those previous calculations approximated the isospin effect by simply dividing the total γ width by a factor of 5 for isospin conjugated nuclei and employed equivalent square well potentials for the calculations of the α transmission coefficients. As expected, differences are larger in comparison to calculations neglecting the isospin suppression.

The statistical model rates are compared with reaction rates derived directly from experiment or calculated from resonance parameters which have been measured through different reaction channels. These rates agree reasonably well with the HF predictions in the astrophysically interesting temperature range $1 < T_9 < 5$ (see Fig. 7). At lower temperatures, the differences tend to be larger, due to the increasing level spacing and the importance of single resonances.

As the isobaric energy shifts are quite different for the considered compound nuclei but the general trend in the isospin suppression of the γ widths is nevertheless well reproduced in the theoretical framework, we conclude that the approach presented here is valid in the energy range of astrophysical importance. The remaining differences have to be attributed to the description of the energy dependence of other nuclear properties, such as the optical α -nucleus potential or the level density.

ACKNOWLEDGMENTS

This work was partly supported by the Swiss NSF (grant 2000-053798.98) and by the National Science Foundation (grant PHY98-03757). T. R. is a PROFIL fellow of the Swiss NSF (grant 2124-055832.98).

TABLES

 TABLE I. Resonance parameters for the $^{20}\text{Ne}(\alpha, \gamma)^{24}\text{Mg}$ reaction.

E_x [MeV]	E_r^{cm} [MeV]	J^π	Γ_{tot} [eV]	$\omega\gamma_{calc}$ [eV]	$\omega\gamma_{exp}$ [eV]
10.111	0.7992	0^+	3.60E-01	2.86E-04	2.90E-04
10.161	0.8492	0^+	3.68E-01	2.30E-05	
10.679	1.3672	0^+	2.29E+00	1.66E-01	1.70E-01
11.457	2.1452	0^+	1.01E+03	2.00E-02	2.00E-02
11.727	2.4152	0^+	1.00E+04	3.70E-01	3.70E-01
13.04	3.7282	0^+	2.30E+03	6.71E-01	7.30E-01
13.198	3.8862	0^+	2.70E+03	4.83E-01	
10.362	1.0502	1^-	4.06E-01	4.91E-04	4.80E-04
10.659	1.3472	1^-	4.93E-01	7.25E-02	
11.39	2.0782	1^-	5.00E+02	4.60E-01	4.60E-01
11.864	2.5522	1^-	7.00E+03	2.40E+00	1.00E+00
12.447	3.1352	1^-	5.56E+03	3.97E-05	
13.253	3.9412	1^-	3.60E+04	4.79E-01	
13.273	3.9612	1^-	2.00E+03	1.67E-01	
13.332	4.0202	1^-	3.10E+04	1.21E-01	
13.407	4.0952	1^-	2.80E+03	2.90E+00	2.90E+00
13.581	4.2692	1^-	2.10E+04	2.50E-01	
13.585	4.2732	1^-	8.00E+03	6.60E-01	
13.81	4.4982	1^-	2.40E+04	2.87E-01	
14.019	4.7072	1^-	6.20E+03	1.25E+00	1.20E+01
9.4578	0.146	2^+	1.10E-01	1.86E-28	
10.361	1.0489	2^+	5.16E-02	7.52E-03	
10.731	1.4192	2^+	4.97E-03	5.08E-03	
10.917	1.6052	2^+	7.34E+00	2.45E+00	2.20E+00
11.016	1.7042	2^+	1.19E+00	1.48E+00	1.50E+00
11.208	1.8962	2^+	2.56E-03	2.74E-03	
11.293	1.9812	2^+	1.93E-04	6.18E-05	
11.33	2.0182	2^+	1.71E+01	3.06E+00	
11.453	2.1412	2^+	3.24E+01	3.28E+00	1.20E+00
11.519	2.2072	2^+	5.02E+02	7.10E-01	8.00E-01
11.964	2.6522	2^+	2.35E+03	8.58E-01	8.50E-01
11.988	2.6762	2^+	7.61E-01	9.48E-03	
12.181	2.8692	2^+	1.73E+02	1.17E+00	9.00E-01
12.403	3.0912	2^+	3.90E+02	6.09E-02	
12.467	3.1552	2^+	3.84E+03	2.11E+00	2.30E+00
12.577	3.2652	2^+	6.43E+03	1.08E+00	9.00E-01
12.737	3.4252	2^+	7.81E+03	1.64E+00	7.00E-01
12.776	3.4642	2^+	3.11E+04	8.67E-03	

12.805	3.4932	2 ⁺	1.09E+03	2.10E+00	1.80E+00
12.845	3.5332	2 ⁺	2.00E+02	2.02E-01	
13.03	3.7182	2 ⁺	1.80E+03	2.85E-03	
13.08	3.7682	2 ⁺	1.19E+04	2.05E+00	2.00E+00
13.137	3.8252	2 ⁺	5.43E+03	6.60E+00	
13.417	4.1052	2 ⁺	4.50E+03	5.58E-03	
13.451	4.1392	2 ⁺	2.10E+03	6.19E-02	
13.473	4.1612	2 ⁺	1.00E+03	2.24E-03	
13.675	4.3632	2 ⁺	5.40E+03	3.83E-01	
13.72	4.4082	2 ⁺	2.74E+03	1.13E+00	
13.884	4.5722	2 ⁺	4.80E+04	1.70E+00	
14.024	4.7122	2 ⁺	7.00E+03	2.66E-03	
14.099	4.7872	2 ⁺	1.40E+03	1.30E+00	1.30E+00
9.532	0.2202	3 ⁻	2.68E-01	1.42E-22	
10.333	1.0212	3 ⁻	4.01E-01	3.21E-04	3.00E-04
10.659	1.3472	3 ⁻	4.69E-01	1.08E-02	
11.162	1.8502	3 ⁻	6.21E-01	2.12E-01	2.20E-01
11.595	2.2832	3 ⁻	1.60E-01	3.55E-02	3.70E-02
11.998	2.6862	3 ⁻	8.68E+00	3.41E-01	3.75E-01
12.015	2.7032	3 ⁻	7.15E+02	5.95E+00	
12.257	2.9452	3 ⁻	1.23E+03	6.32E+00	
12.659	3.3472	3 ⁻	9.01E+02	5.05E+00	
12.919	3.6072	3 ⁻	6.67E+03	7.19E-01	
13.087	3.7752	3 ⁻	8.96E+03	2.54E-01	
13.423	4.1112	3 ⁻	4.51E+03	5.14E-01	
13.445	4.1332	3 ⁻	2.00E+02	1.05E-01	
10.581	1.2692	4 ⁺	4.51E-01	6.37E-04	
10.66	1.3482	4 ⁺	4.68E-01	1.67E-03	
11.217	1.9052	4 ⁺	8.72E-01	1.67E+00	1.70E+00
11.314	2.0022	4 ⁺	6.81E-01	4.25E-01	
11.695	2.3832	4 ⁺	1.60E+00	1.12E+00	1.10E+00
12.049	2.7372	4 ⁺	2.74E-01	4.68E-01	
12.117	2.8052	4 ⁺	1.90E+03	1.41E+00	1.40E+00
12.161	2.8492	4 ⁺	9.00E+02	7.18E-01	
12.504	3.1922	4 ⁺	1.73E+02	6.15E+00	6.20E+00
12.636	3.3242	4 ⁺	3.00E+01	8.67E-01	
12.972	3.6602	4 ⁺	3.30E+03	9.67E-02	
13.05	3.7382	4 ⁺	9.06E+01	5.78E+00	
14.148	4.8362	4 ⁺	1.80E+03	1.25E+00	1.50E+00
14.327	5.0152	4 ⁺	9.02E+03	6.68E+00	6.40E+00

TABLE II. Resonance parameters for the $^{24}\text{Mg}(\alpha, \gamma)^{28}\text{Si}$ reaction.

E_x [MeV]	E_r^{cm} [MeV]	J^π	Γ_{tot} [eV]	$\omega\gamma_{calc}$ [eV]	$\omega\gamma_{exp}$ [eV]
12.976	2.992	0^+	5.20E+03	5.25E-02	
13.039	3.055	0^+	3.20E+03	1.77E-01	3.00E-01
13.235	3.251	0^+	3.00E+03	3.53E-01	1.30E+00
11.295	1.311	1^-	9.50E-02	9.08E-03	1.10E-01
11.669	1.685	1^-	4.60E-01	2.13E-01	3.30E-01
12.181	2.197	1^-	8.26E+00	9.47E-02	1.00E-01
12.3	2.316	1^-	2.20E+01	2.19E-02	2.00E-02
12.815	2.831	1^-	3.50E+03	5.17E-01	2.00E-01
12.973	2.989	1^-	1.69E+03	1.77E+01	8.00E-01
13.423	3.439	1^-	1.97E+04	1.72E+01	
13.734	3.75	1^-	3.50E+04	4.77E-02	
13.812	3.828	1^-	3.70E+03	4.83E-01	3.00E-01
13.897	3.913	1^-	5.40E+03	5.28E-01	
13.986	4.002	1^-	2.71E+03	2.18E-02	
10.209	0.225	2^+	3.39E-02	2.17E-26	
10.514	0.53	2^+	6.42E-02	2.18E-12	
10.805	0.821	2^+	7.36E-02	2.74E-07	
10.915	0.931	2^+	7.75E-02	4.99E-06	
10.994	1.01	2^+	3.13E-02	2.95E-05	
10.951	0.967	2^+	7.88E-02	1.15E-05	
11.078	1.094	2^+	8.35E-02	1.56E-04	
11.138	1.154	2^+	8.58E-02	4.58E-04	
11.265	1.281	2^+	9.14E-02	3.39E-03	
11.432	1.448	2^+	1.04E-01	2.94E-02	
11.515	1.531	2^+	1.17E-01	6.99E-02	6.00E-02
11.656	1.672	2^+	1.80E-01	2.13E-01	1.40E-01
11.778	1.794	2^+	2.16E-01	2.72E-02	3.00E-02
12.071	2.087	2^+	2.18E+00	5.51E-01	3.60E-01
12.289	2.305	2^+	2.10E+01	1.01E-01	9.00E-02
12.44	2.456	2^+	1.76E+01	1.70E+00	1.00E+00
12.714	2.73	2^+	5.01E+01	2.14E-04	
12.725	2.741	2^+	6.43E+02	1.27E+00	3.60E+00
12.754	2.77	2^+	5.07E+01	6.02E-02	
12.899	2.915	2^+	9.59E+02	5.20E+00	2.40E+00
12.923	2.939	2^+	2.31E+02	5.58E-01	4.00E-01
13.105	3.121	2^+	2.47E+02	2.84E+00	2.10E+00
13.187	3.203	2^+	1.90E+03	1.85E-02	
13.203	3.219	2^+	2.14E+02	1.23E-01	
13.228	3.244	2^+	2.25E+02	1.12E+00	1.30E+00
13.42	3.436	2^+	1.12E+03	4.32E-01	3.70E-01

13.461	3.477	2 ⁺	1.80E+03	3.90E-01	
13.482	3.498	2 ⁺	1.53E+03	1.03E-01	
13.545	3.561	2 ⁺	8.47E+03	2.71E-02	
13.638	3.654	2 ⁺	4.50E+03	5.12E-02	9.00E-02
13.639	3.655	2 ⁺	1.20E+02	6.68E-01	
13.677	3.693	2 ⁺	1.37E+03	1.41E+00	1.10E+00
13.705	3.721	2 ⁺	5.00E+02	1.66E+00	
13.939	3.955	2 ⁺	5.17E+03	3.93E+00	6.00E-02
13.971	3.987	2 ⁺	2.52E+03	1.86E+00	6.00E-01
13.983	3.999	2 ⁺	3.84E+02	1.80E+01	
14.064	4.08	2 ⁺	6.00E+03	5.77E-01	8.00E-01
14.309	4.325	2 ⁺	2.00E+04	5.11E+00	2.00E+00
10.181	0.197	3 ⁻	1.00E-01	8.12E-30	
10.54	0.556	3 ⁻	6.50E-02	2.17E-12	
11.584	1.6	3 ⁻	1.10E-01	3.93E-02	4.00E-02
11.899	1.915	3 ⁻	1.00E+02	6.37E-02	6.00E-03
11.931	1.947	3 ⁻	3.27E-01	4.32E-01	
11.975	1.991	3 ⁻	7.00E-01	1.43E-01	1.00E-01
12.134	2.15	3 ⁻	1.00E+01	6.48E-02	
12.193	2.209	3 ⁻	2.32E+01	1.56E-01	1.90E-01
12.488	2.504	3 ⁻	1.09E+02	1.88E-01	2.00E-01
12.741	2.757	3 ⁻	2.00E+03	1.87E-03	
12.801	2.817	3 ⁻	9.72E+01	8.60E-03	
12.858	2.874	3 ⁻	2.00E+02	5.33E-01	6.00E-01
12.989	3.005	3 ⁻	2.30E+03	1.28E-02	
13.114	3.13	3 ⁻	1.52E+04	6.70E-03	
13.172	3.188	3 ⁻	3.06E+02	9.01E-02	
13.246	3.262	3 ⁻	9.97E+03	2.16E-01	2.00E-01
13.317	3.333	3 ⁻	1.20E+03	1.77E-01	
13.358	3.374	3 ⁻	4.72E+03	2.07E-01	2.30E-01
13.491	3.507	3 ⁻	3.20E+04	4.93E-02	
13.662	3.678	3 ⁻	4.50E+02	3.62E-01	
13.711	3.727	3 ⁻	2.00E+04	2.03E-01	8.00E-01
13.788	3.804	3 ⁻	2.70E+03	3.32E-01	
13.835	3.851	3 ⁻	9.00E+02	3.39E-01	1.00E-01
13.859	3.875	3 ⁻	3.87E+03	3.27E+00	
13.872	3.888	3 ⁻	7.10E+03	9.05E-01	8.00E-01

TABLE III. Resonance parameters for the $^{28}\text{Si}(\alpha, \gamma)^{32}\text{S}$ reaction.

E_x [MeV]	E_r^{cm} [MeV]	J^π	Γ_{tot} [eV]	$\omega\gamma_{calc}$ [eV]	$\omega\gamma_{exp}$ [eV]
8.507	1.558	0^+	2.25E-02	2.61E-04	
9.983	3.034	0^+	1.19E+02	1.11E-01	
10.457	3.508	0^+	1.73E+03	1.72E-02	
10.787	3.838	0^+	6.00E+02	4.50E+01	
11.064	4.115	0^+	1.25E+04	1.34E-03	
11.584	4.635	0^+	3.19E+03	7.66E-02	
11.607	4.658	0^+	3.10E+02	8.52E+00	
11.869	4.92	0^+	1.10E+03	7.13E-02	
11.93	4.981	0^+	1.00E+02	4.93E-01	
7.434	0.485	1^-	1.14E-02	5.03E-18	
8.494	1.545	1^-	2.91E-02	1.59E-02	1.60E-02
9.236	2.287	1^-	8.99E-01	5.94E-01	5.40E-01
9.486	2.537	1^-	9.98E+00	4.48E-02	8.30E-01
9.731	2.782	1^-	3.74E+02	1.85E-03	
9.849	2.9	1^-	1.02E+02	8.99E-03	
9.95	3.001	1^-	1.50E+02	5.48E-02	
10.226	3.277	1^-	1.80E+02	1.48E-02	
10.332	3.383	1^-	6.64E+03	4.82E-02	
10.604	3.655	1^-	1.50E+02	2.55E-01	
10.701	3.752	1^-	2.10E+04	2.23E-01	
10.711	3.762	1^-	2.00E+04	3.21E+00	2.70E+00
10.826	3.877	1^-	2.26E+04	2.38E-02	
10.916	3.967	1^-	1.63E+03	1.56E-01	
11.234	4.285	1^-	7.90E+03	1.42E-02	
11.447	4.498	1^-	5.30E+03	1.00E-02	
11.587	4.638	1^-	1.64E+03	2.91E-01	
11.609	4.66	1^-	1.93E+04	2.13E-02	
11.63	4.681	1^-	2.71E+04	2.09E-02	
11.735	4.786	1^-	2.43E+04	1.81E-02	
11.807	4.858	1^-	3.71E+04	3.43E-02	
11.91	4.961	1^-	6.30E+03	4.32E-01	
12.185	5.236	1^-	1.07E+04	5.62E-02	
12.195	5.246	1^-	5.63E+03	3.60E-02	
12.296	5.347	1^-	1.56E+04	2.21E-02	
12.336	5.387	1^-	2.80E+03	8.08E-03	
12.39	5.441	1^-	4.20E+03	1.63E-03	
7.484	0.535	2^+	1.17E-02	9.52E-17	
8.344	1.395	2^+	2.02E-02	3.20E-05	
8.69	1.741	2^+	2.74E-02	1.17E-02	1.20E-02
8.861	1.912	2^+	3.15E-02	1.82E-02	1.60E-02

9.196	2.247	2 ⁺	4.45E-01	1.52E-01	
9.464	2.515	2 ⁺	8.59E-01	7.12E-01	7.20E-01
9.65	2.701	2 ⁺	7.46E+00	9.53E-02	
9.711	2.762	2 ⁺	4.68E+00	2.91E-01	6.30E-01
9.817	2.868	2 ⁺	6.82E+00	6.21E-03	
9.92	2.971	2 ⁺	1.00E+01	3.68E-02	
10.293	3.344	2 ⁺	7.00E+01	2.52E-02	
10.51	3.561	2 ⁺	1.00E+01	1.66E-02	
10.528	3.579	2 ⁺	8.01E+01	7.41E-02	7.00E-02
10.696	3.747	2 ⁺	1.80E+02	1.01E-01	
10.757	3.808	2 ⁺	5.00E+01	1.32E-01	
10.779	3.83	2 ⁺	6.00E+02	3.69E-01	
10.792	3.843	2 ⁺	1.76E+02	1.33E+00	
10.827	3.878	2 ⁺	3.21E+02	5.35E+00	
10.933	3.984	2 ⁺	4.80E+01	3.57E-01	
11.051	4.102	2 ⁺	4.22E+03	1.66E-02	
11.083	4.134	2 ⁺	8.50E+01	2.11E-01	
11.237	4.288	2 ⁺	5.00E+01	2.12E-01	
11.255	4.306	2 ⁺	2.10E+02	2.64E-01	
11.333	4.384	2 ⁺	1.50E+02	2.23E-01	
11.487	4.538	2 ⁺	5.04E+02	6.57E-02	
11.604	4.655	2 ⁺	8.10E+02	6.73E-03	
11.679	4.73	2 ⁺	2.60E+03	2.50E-02	
11.722	4.773	2 ⁺	2.81E+03	1.00E-02	
11.832	4.883	2 ⁺	1.40E+02	1.35E-01	
12.00	5.051	2 ⁺	2.00E+03	3.69E-03	
12.014	5.065	2 ⁺	9.01E+03	1.52E-01	
12.022	5.073	2 ⁺	2.63E+03	4.93E-02	
12.147	5.198	2 ⁺	1.32E+04	4.93E-02	
12.298	5.349	2 ⁺	3.26E+02	6.27E-01	
12.389	5.44	2 ⁺	1.85E+03	1.57E-01	
12.399	5.45	2 ⁺	3.61E+02	3.28E-01	
12.473	5.524	2 ⁺	1.40E+03	5.95E-03	
7.701	0.752	3 ⁻	1.35E-02	1.64E-12	
9.023	2.074	3 ⁻	4.02E-02	5.36E-02	5.20E-02
9.464	2.515	3 ⁻	1.07E-01	1.61E-01	
9.724	2.775	3 ⁻	1.59E+00	1.57E-02	
9.817	2.868	3 ⁻	4.15E+00	7.33E-03	
10.223	3.274	3 ⁻	6.36E+01	7.65E+00	8.10E+00
10.288	3.339	3 ⁻	1.62E+02	2.19E+00	2.30E+00
10.626	3.677	3 ⁻	6.68E+02	4.65E-01	6.00E-01
11.092	4.143	3 ⁻	7.00E+01	2.93E-01	
11.197	4.248	3 ⁻	8.00E+01	3.44E-01	
11.231	4.282	3 ⁻	8.00E+02	3.78E-02	

11.557	4.608	3 ⁻	5.00E+01	2.74E-01
11.625	4.676	3 ⁻	6.00E+01	2.68E-01
11.758	4.809	3 ⁻	1.40E+02	1.54E-01
11.784	4.835	3 ⁻	3.00E+01	7.60E-01
11.805	4.856	3 ⁻	2.02E+03	7.98E-03
11.879	4.93	3 ⁻	3.60E+03	3.86E-02
11.902	4.953	3 ⁻	2.45E+03	3.74E-02
11.936	4.987	3 ⁻	1.48E+03	4.73E-02
12.143	5.194	3 ⁻	3.20E+03	1.59E-03
12.154	5.205	3 ⁻	4.45E+03	5.84E-02
12.272	5.323	3 ⁻	3.08E+02	8.98E-01
12.421	5.472	3 ⁻	2.85E+03	3.28E-01
12.457	5.508	3 ⁻	3.38E+03	1.41E-02

TABLE IV. Resonance parameters for the $^{32}\text{S}(\alpha, \gamma)^{36}\text{Ar}$ reaction.

E_x [MeV]	E_r^{cm} [MeV]	J^π	Γ_{tot} [eV]	$\omega\gamma_{calc}$ [eV]	$\omega\gamma_{exp}$ [eV]
7.136	0.495	1 ⁻	5.00E-02	4.30E-21	
7.247	0.606	1 ⁻	3.00E-02	1.43E-17	
7.749	1.108	1 ⁻	1.62E-02	4.83E-09	
7.879	1.238	1 ⁻	1.76E-02	9.37E-08	
8.302	1.661	1 ⁻	2.29E-02	2.06E-04	
9.117	2.476	1 ⁻	1.16E+00	2.73E-01	3.00E-01
9.366	2.725	1 ⁻	1.38E+01	2.38E-01	
9.702	3.061	1 ⁻	1.74E+01	3.43E-02	
9.811	3.17	1 ⁻	3.10E+01	7.99E-02	
9.982	3.341	1 ⁻	6.29E+01	2.51E-02	
10.044	3.403	1 ⁻	7.38E+02	1.40E-01	2.30E-01
10.099	3.458	1 ⁻	4.01E+02	2.36E-01	
10.142	3.501	1 ⁻	1.47E+02	6.71E-01	
10.173	3.532	1 ⁻	1.10E+03	1.14E-02	
10.186	3.545	1 ⁻	1.08E+03	1.71E-01	3.00E-01
10.267	3.626	1 ⁻	9.00E+02	5.56E-03	
10.499	3.858	1 ⁻	2.50E+03	6.01E-02	
10.635	3.994	1 ⁻	4.10E+03	1.42E-01	
10.65	4.009	1 ⁻	1.50E+03	3.44E-01	3.20E-01
10.683	4.042	1 ⁻	6.20E+03	2.36E-03	
10.701	4.06	1 ⁻	5.07E+02	3.57E-02	
10.831	4.19	1 ⁻	5.64E+02	4.84E-03	
6.73	0.089	2 ⁺	8.01E-03	4.03E-71	
6.867	0.226	2 ⁺	8.86E-03	1.13E-38	
7.178	0.537	2 ⁺	1.11E-02	1.55E-19	
7.423	0.782	2 ⁺	1.31E-02	1.58E-13	
7.97	1.329	2 ⁺	1.87E-02	7.62E-07	
8.555	1.914	2 ⁺	2.71E-02	2.79E-03	
8.909	2.268	2 ⁺	4.00E-02	2.99E-02	3.00E-02
9.144	2.503	2 ⁺	2.39E-01	3.20E-02	
9.356	2.715	2 ⁺	2.69E+00	4.58E-02	5.00E-02
9.373	2.732	2 ⁺	3.48E+00	5.03E-02	
9.439	2.798	2 ⁺	1.01E+01	2.06E-01	
9.448	2.807	2 ⁺	5.84E+00	1.04E-02	
9.464	2.823	2 ⁺	6.36E+00	9.70E-03	
9.502	2.861	2 ⁺	8.74E+00	1.28E-02	
9.595	2.954	2 ⁺	1.92E+01	7.24E-02	
9.878	3.237	2 ⁺	9.83E+01	5.97E-02	
9.956	3.315	2 ⁺	1.10E+02	9.00E-02	
9.9951	3.3541	2 ⁺	5.02E+01	3.29E-01	
10.095	3.454	2 ⁺	1.79E+02	2.43E-03	

10.217	3.576	2 ⁺	3.10E+02	5.02E-02	5.00E-02
10.319	3.678	2 ⁺	3.65E+02	3.18E-02	
10.328	3.687	2 ⁺	3.68E+02	1.11E-02	
10.346	3.705	2 ⁺	3.86E+02	1.16E-02	
10.439	3.798	2 ⁺	5.23E+02	3.85E-02	5.00E-01
10.588	3.947	2 ⁺	6.71E+02	1.68E-02	
10.593	3.952	2 ⁺	6.91E+02	2.64E-02	
10.7	4.059	2 ⁺	2.80E+02	4.08E-01	
10.789	4.148	2 ⁺	1.83E+03	6.08E-04	
10.851	4.21	2 ⁺	1.07E+03	2.49E-02	
6.836	0.195	3 ⁻	2.74E-03	4.16E-41	
7.258	0.617	3 ⁻	1.17E-02	2.17E-15	
7.627	0.986	3 ⁻	1.50E-02	1.52E-08	
7.749	1.108	3 ⁻	1.62E-02	4.38E-07	
8.352	1.711	3 ⁻	2.67E-02	1.92E-02	
8.472	1.831	3 ⁻	2.85E-02	4.96E-02	
8.672	2.031	3 ⁻	2.90E-02	3.89E-03	
8.806	2.165	3 ⁻	3.12E-02	2.73E-03	
9.066	2.425	3 ⁻	1.98E-01	4.07E-03	
9.132	2.491	3 ⁻	1.38E-01	4.91E-02	
9.192	2.551	3 ⁻	5.29E-01	2.00E-01	
9.24	2.599	3 ⁻	4.39E-01	1.36E-01	
9.258	2.617	3 ⁻	5.13E-01	1.33E-01	
9.509	2.868	3 ⁻	4.23E+00	2.10E-01	
9.737	3.096	3 ⁻	4.00E+02	1.48E-03	
9.764	3.123	3 ⁻	2.87E+01	2.66E-01	
9.982	3.341	3 ⁻	5.90E+01	9.21E-02	
10.05	3.409	3 ⁻	3.97E+02	8.58E-02	
10.167	3.526	3 ⁻	8.70E+02	8.94E-03	
10.255	3.614	3 ⁻	1.18E+03	1.18E-02	
10.28	3.639	3 ⁻	1.25E+03	9.13E-05	
10.308	3.667	3 ⁻	5.40E+02	2.81E-02	
10.42	3.779	3 ⁻	4.70E+03	4.31E-02	
10.488	3.847	3 ⁻	2.04E+02	4.92E-01	9.00E-01
10.539	3.898	3 ⁻	2.59E+03	1.27E-01	
10.596	3.955	3 ⁻	4.57E+03	1.98E-01	3.00E-01
10.674	4.033	3 ⁻	1.75E+02	9.08E-03	
10.853	4.212	3 ⁻	2.88E+02	5.07E-01	1.10E-01

TABLE V. Resonance parameters for the $^{36}\text{Ar}(\alpha, \gamma)^{40}\text{Ca}$ reaction.

E_x [MeV]	E_r^{cm} [MeV]	J^π	Γ_{tot} [eV]	$\omega\gamma_{calc}$ [eV]	$\omega\gamma_{exp}$ [eV]
7.3	0.259	0^+	3.80E-03	9.85E-40	
7.701	0.66	0^+	4.88E-02	2.55E-18	
7.814	0.773	0^+	5.24E-02	5.26E-16	
8.018	0.977	0^+	5.96E-02	2.24E-12	
8.27	1.229	0^+	6.96E-02	3.18E-09	
8.439	1.398	0^+	7.70E-02	6.19E-08	
8.484	1.443	0^+	1.90E-02	1.61E-07	
8.938	1.897	0^+	1.03E-01	5.53E-05	
9.304	2.263	0^+	2.15E-01	1.61E-03	
10.42	3.379	0^+	4.55E+01	1.87E-01	
12.27	5.229	0^+	4.10E+03	1.07E-01	
7.113	0.072	1^-	8.20E-03	1.13E-90	
8.113	1.072	1^-	1.19E-02	2.20E-10	
8.271	1.23	1^-	6.97E-02	6.07E-09	
8.323	1.282	1^-	8.20E-03	2.04E-08	
8.358	1.317	1^-	4.40E-03	4.43E-08	
8.665	1.624	1^-	8.80E-02	6.27E-06	
8.994	1.953	1^-	7.01E-02	2.33E-03	
9.432	2.391	1^-	2.30E+02	6.58E-05	
9.538	2.497	1^-	4.00E+02	5.12E-06	
9.604	2.563	1^-	1.90E+02	4.18E-04	
10.199	3.158	1^-	2.70E+02	8.04E-04	
10.267	3.226	1^-	1.77E+02	7.06E-04	
10.278	3.237	1^-	1.03E+03	8.70E-04	
10.421	3.38	1^-	5.94E+02	4.70E-03	
10.623	3.582	1^-	5.00E+03	6.78E-04	
10.67	3.629	1^-	5.70E+03	1.48E-04	
10.91	3.869	1^-	2.30E+03	1.42E-02	
10.951	3.91	1^-	1.00E+04	3.47E-02	
11.022	3.981	1^-	2.71E+02	2.92E-01	
12.099	5.058	1^-	1.09E+03	1.50E-01	1.00E-01
12.944	5.903	1^-	3.78E+03	1.12E+00	3.40E+00
13.245	6.204	1^-	9.30E+03	1.15E+00	9.70E+00
13.442	6.401	1^-	5.63E+03	1.52E+00	3.40E+00
13.784	6.743	1^-	7.07E+03	1.83E+00	3.70E+00
13.956	6.915	1^-	2.40E+04	1.47E+01	1.46E+01
14.08	7.039	1^-	1.43E+04	1.69E+01	1.44E+01
14.42	7.379	1^-	1.71E+04	2.83E+00	4.70E+00
14.51	7.469	1^-	1.79E+04	2.93E+00	4.50E+00
14.87	7.829	1^-	2.09E+04	3.36E+00	6.30E+00

7.277	0.236	2 ⁺	9.30E-03	3.36E-43
7.446	0.405	2 ⁺	5.90E-02	8.90E-28
7.676	0.635	2 ⁺	2.00E-03	1.85E-19
7.872	0.831	2 ⁺	2.25E-01	6.39E-15
7.976	0.935	2 ⁺	1.00E-02	7.85E-13
8.091	1.05	2 ⁺	1.48E-01	3.77E-11
8.338	1.297	2 ⁺	7.25E-02	2.92E-08
8.578	1.537	2 ⁺	9.30E-02	3.69E-06
8.748	1.707	2 ⁺	6.50E-02	5.58E-05
8.934	1.893	2 ⁺	2.58E-01	2.95E-04
8.981	1.94	2 ⁺	5.40E-02	5.72E-04
9.227	2.186	2 ⁺	4.97E+00	3.94E-04
9.388	2.347	2 ⁺	2.11E+01	3.86E-04
10.54	3.499	2 ⁺	5.07E+02	1.96E-02
10.691	3.65	2 ⁺	1.40E+02	2.53E-02
10.78	3.739	2 ⁺	1.80E+02	1.79E-02
10.862	3.821	2 ⁺	4.53E+01	1.21E-01
11.042	4.001	2 ⁺	5.00E+02	1.45E-02
11.117	4.076	2 ⁺	3.18E+01	3.68E+00
11.266	4.225	2 ⁺	3.40E+02	1.20E+00
11.324	4.283	2 ⁺	5.76E+02	2.77E-01
11.369	4.328	2 ⁺	2.47E+02	8.29E-01
11.459	4.418	2 ⁺	1.31E+03	5.38E-01
7.239	0.198	3 ⁻	4.66E-03	2.10E-49
7.623	0.582	3 ⁻	4.07E-03	9.94E-22
7.769	0.728	3 ⁻	2.72E-03	2.25E-16
8.764	1.723	3 ⁻	9.65E-02	2.60E-05
9.091	2.05	3 ⁻	1.25E-01	9.54E-04
9.362	2.321	3 ⁻	1.27E+00	2.49E-03
9.453	2.412	3 ⁻	9.00E+01	5.87E-05
10.13	3.089	3 ⁻	7.32E+01	2.17E-02
10.262	3.221	3 ⁻	3.74E+02	8.56E-04
10.361	3.32	3 ⁻	3.90E+03	7.92E-05
10.443	3.402	3 ⁻	4.40E+02	1.09E-02
10.776	3.735	3 ⁻	1.20E+03	1.07E-01
11.011	3.97	3 ⁻	2.76E+02	7.93E-02
11.249	4.208	3 ⁻	8.47E+02	8.40E-02

TABLE VI. Resonance parameters for the $^{40}\text{Ca}(\alpha, \gamma)^{44}\text{Ti}$ reaction.

E_x [MeV]	E_r^{cm} [MeV]	J^π	Γ_{tot} [eV]	$\omega\gamma_{calc}$ [eV]	$\omega\gamma_{exp}$ [eV]
8.954	3.827	1^-	5.38E-01	2.34E-01	2.20E-01
6.22	1.093	2^+	7.17E-02	2.81E-13	
7.634	2.507	2^+	2.02E-01	1.32E-02	1.30E-02
8.067	2.94	2^+	2.68E-01	2.27E-02	2.20E-02
8.318	3.191	2^+	3.37E-01	1.38E-01	1.20E-01
8.385	3.258	2^+	4.76E-01	5.26E-01	5.20E-01
8.449	3.322	2^+	3.96E-01	2.69E-01	2.80E-01
8.511	3.384	2^+	4.11E-01	2.82E-01	2.20E-01
8.534	3.407	2^+	4.50E-01	3.93E-01	3.30E-01
8.565	3.438	2^+	3.78E-01	1.06E-01	1.10E-01
8.627	3.5	2^+	3.84E-01	7.87E-02	8.00E-02
8.639	3.512	2^+	4.40E-01	2.94E-01	2.30E-01
8.756	3.629	2^+	4.73E-01	3.22E-01	3.30E-01
8.946	3.819	2^+	4.70E-01	1.37E-01	1.10E-01
8.987	3.86	2^+	5.38E-01	3.64E-01	3.00E-01
9.215	4.088	2^+	6.23E-01	4.43E-01	5.00E-01
9.227	4.1	2^+	7.04E+00	5.41E+00	5.80E+00
9.239	4.112	2^+	2.90E+00	2.12E+00	2.00E+00
9.361	4.234	2^+	1.18E+00	1.31E+00	1.20E+00
10.386	5.259	2^+	4.99E+02	4.95E+00	5.00E+00
8.534	3.407	3^-	4.09E-01	3.61E-01	3.30E-01
8.96	3.833	3^-	5.25E-01	4.78E-01	4.00E-01
9.361	4.234	3^-	9.43E-01	1.33E+00	1.20E+00
10.386	5.259	3^-	1.15E+03	4.86E+00	5.00E+00
5.21	0.083	4^+	1.32E-03	2.68E-61	
5.305	0.178	4^+	1.32E-03	2.68E-61	
8.992	3.865	4^+	5.32E-01	6.11E-01	6.00E-01
9.427	4.3	4^+	9.08E-01	8.95E-01	9.00E-01
9.713	4.586	4^+	8.86E+00	2.33E+00	2.50E+00

TABLE VII. Reaction rate for $^{20}\text{Ne}(\alpha, \gamma)^{24}\text{Mg}$ as a function of temperature. Listed are the rates calculated on the basis of measured resonances, and of the predicted resonances using the parameters given in table I. For comparison also shown is the rate predicted with the statistical model code NON-SMOKER.

Temperature [GK]	$N_A < \sigma v >_{exp}$ [cm 3 s $^{-1}$ mole $^{-1}$]	$N_A < \sigma v >_{emp}$ [cm 3 s $^{-1}$ mole $^{-1}$]	$N_A < \sigma v >_{HF}$ [cm 3 s $^{-1}$ mole $^{-1}$]
.1000	1.40E-38	9.13E-28	5.77E-25
.1500	1.94E-25	2.65E-24	2.55E-19
.2000	6.38E-19	5.89E-19	6.48E-16
.3000	1.75E-12	1.67E-12	1.10E-11
.4000	2.56E-09	2.53E-09	4.58E-09
.5000	1.90E-07	2.01E-07	3.02E-07
.6000	3.25E-06	3.88E-06	6.77E-06
.7000	2.50E-05	3.50E-05	7.46E-05
.8000	1.26E-04	2.03E-04	5.01E-04
.9000	5.22E-04	9.04E-04	2.35E-03
1.0000	1.94E-03	3.34E-03	8.49E-03
1.5000	2.47E-01	3.36E-01	5.35E-01
2.0000	3.43E+00	4.43E+00	5.33E+00
3.0000	4.60E+01	6.28E+01	6.60E+01
4.0000	1.58E+02	2.39E+02	2.58E+02
5.0000	3.16E+02	5.35E+02	6.06E+02
6.0000	4.83E+02	9.13E+02	1.09E+03
7.0000	6.37E+02	1.33E+03	1.66E+03
8.0000	7.67E+02	1.76E+03	2.28E+03
9.0000	8.70E+02	2.16E+03	2.92E+03
10.0000	9.48E+02	2.54E+03	3.55E+03

TABLE VIII. Reaction rate for $^{24}\text{Mg}(\alpha, \gamma)^{28}\text{Si}$ as a function of temperature. Listed are the rates calculated on the basis of measured resonances, and of the predicted resonances using the parameters given in table II. For comparison also shown is the rate predicted with the statistical model code NON-SMOKER.

Temperature [GK]	$N_A < \sigma v >_{exp}$ [cm 3 s $^{-1}$ mole $^{-1}$]	$N_A < \sigma v >_{emp}$ [cm 3 s $^{-1}$ mole $^{-1}$]	$N_A < \sigma v >_{HF}$ [cm 3 s $^{-1}$ mole $^{-1}$]
.1000	0.00E+00	8.02E-32	7.85E-30
.1500	4.52E-37	1.61E-24	2.08E-23
.2000	1.90E-27	3.19E-20	1.60E-19
.3000	6.85E-18	1.53E-15	1.13E-14
.4000	3.82E-13	4.11E-12	1.22E-11
.5000	2.68E-10	1.19E-09	1.64E-09
.6000	2.16E-08	8.62E-08	6.44E-08
.7000	5.17E-07	2.19E-06	1.13E-06
.8000	5.87E-06	2.60E-05	1.13E-05
.9000	4.09E-05	1.80E-04	7.45E-05
1.0000	2.02E-04	8.54E-04	3.58E-04
1.5000	3.24E-02	9.50E-02	5.73E-02
2.0000	4.80E-01	1.06E+00	9.14E-01
3.0000	8.42E+00	1.34E+01	1.71E+01
4.0000	3.98E+01	5.49E+01	7.86E+01
5.0000	1.05E+02	1.43E+02	2.00E+02
6.0000	1.99E+02	2.86E+02	1.83E+02
7.0000	3.11E+02	4.79E+02	5.95E+02
8.0000	4.27E+02	7.09E+02	8.47E+02
9.0000	5.40E+02	9.59E+02	1.12E+03
10.0000	6.42E+02	1.21E+03	1.41E+03

TABLE IX. Reaction rate for $^{28}\text{Si}(\alpha, \gamma)^{32}\text{S}$ as a function of temperature. Listed are the rates calculated on the basis of measured resonances, and of the predicted resonances using the parameters given in table III. For comparison also shown is the rate predicted with the statistical model code NON-SMOKER.

Temperature [GK]	$N_A < \sigma v >_{exp}$ [cm 3 s $^{-1}$ mole $^{-1}$]	$N_A < \sigma v >_{emp}$ [cm 3 s $^{-1}$ mole $^{-1}$]	$N_A < \sigma v >_{HF}$ [cm 3 s $^{-1}$ mole $^{-1}$]
.1000	0.00E+00	1.42E-36	2.20E-34
.1500	0.00E+00	1.44E-28	3.14E-27
.2000	4.90E-36	1.67E-24	6.94E-23
.3000	2.54E-23	7.37E-20	1.83E-17
.4000	5.09E-17	1.12E-16	4.64E-14
.5000	2.86E-13	3.11E-13	1.17E-11
.6000	8.67E-11	9.09E-11	7.45E-10
.7000	4.98E-09	5.16E-09	1.91E-08
.8000	1.02E-07	1.05E-07	2.60E-07
.9000	1.06E-06	1.08E-06	2.20E-06
1.0000	6.80E-06	6.97E-06	1.30E-05
1.5000	1.90E-03	1.98E-03	4.13E-03
2.0000	4.00E-02	4.23E-02	9.84E-02
3.0000	1.34E+00	1.45E+00	3.04E+00
4.0000	9.39E+00	1.16E+01	1.90E+01
5.0000	3.15E+01	4.65E+01	5.97E+01
6.0000	7.07E+01	1.22E+02	1.31E+02
7.0000	1.24E+02	2.45E+02	2.35E+02
8.0000	1.87E+02	4.11E+02	3.67E+02
9.0000	2.54E+02	6.07E+02	5.24E+02
10.0000	3.20E+02	8.21E+02	7.01E+02

TABLE X. Reaction rate for $^{32}\text{S}(\alpha, \gamma)^{36}\text{Ar}$ as a function of temperature. Listed are the rates calculated on the basis of measured resonances, and of the predicted resonances using the parameters given in table IV. For comparison also shown is the rate predicted with the statistical model code NON-SMOKER.

Temperature [GK]	$N_A < \sigma v >_{exp}$ [cm 3 s $^{-1}$ mole $^{-1}$]	$N_A < \sigma v >_{emp}$ [cm 3 s $^{-1}$ mole $^{-1}$]	$N_A < \sigma v >_{HF}$ [cm 3 s $^{-1}$ mole $^{-1}$]
.1000	0.00E+00	5.78E-40	3.70E-39
.1500	0.00E+00	1.71E-30	2.64E-31
.2000	0.00E+00	1.63E-25	1.60E-26
.3000	4.55E-35	8.78E-20	1.50E-20
.4000	1.04E-25	9.70E-16	8.52E-17
.5000	4.12E-20	3.21E-13	3.86E-14
.6000	2.18E-16	2.03E-11	3.93E-12
.7000	9.95E-14	7.43E-10	1.51E-10
.8000	9.86E-12	1.72E-08	2.91E-09
.9000	3.53E-10	2.25E-07	3.39E-08
1.0000	6.19E-09	1.81E-06	2.70E-07
1.5000	3.30E-05	9.43E-04	2.41E-04
2.0000	2.32E-03	2.22E-02	9.64E-03
3.0000	1.53E-01	6.44E-01	4.56E-01
4.0000	1.23E+00	4.02E+00	3.42E+00
5.0000	4.34E+00	1.26E+01	1.23E+01
6.0000	1.01E+01	2.71E+01	3.07E+01
7.0000	1.84E+01	4.65E+01	6.25E+01
8.0000	2.88E+01	6.91E+01	1.12E+02
9.0000	4.03E+01	9.29E+01	1.81E+02
10.0000	5.22E+01	1.17E+02	2.73E+02

TABLE XI. Reaction rate for $^{36}\text{Ar}(\alpha, \gamma)^{40}\text{Ca}$ as a function of temperature. Listed are the rates calculated on the basis of measured resonances, and of the predicted resonances using the parameters given in table V. For comparison also shown is the rate predicted with the statistical model code NON-SMOKER.

Temperature [GK]	$N_A < \sigma v >_{exp}$ [cm 3 s $^{-1}$ mole $^{-1}$]	$N_A < \sigma v >_{emp}$ [cm 3 s $^{-1}$ mole $^{-1}$]	$N_A < \sigma v >_{HF}$ [cm 3 s $^{-1}$ mole $^{-1}$]
.1000	0.00E+00	2.46E-42	2.07E-43
.1500	0.00E+00	1.51E-34	6.84E-35
.2000	0.00E+00	5.27E-29	1.08E-29
.3000	0.00E+00	1.18E-22	3.41E-23
.4000	0.00E+00	1.71E-18	4.08E-19
.5000	0.00E+00	1.21E-15	3.12E-16
.6000	2.80E-45	1.55E-13	4.85E-14
.7000	2.67E-38	7.33E-12	2.52E-12
.8000	4.85E-33	1.76E-10	5.83E-11
.9000	5.93E-29	2.42E-09	7.44E-10
1.0000	1.10E-25	2.11E-08	6.07E-09
1.5000	6.67E-16	1.71E-05	4.91E-06
2.0000	5.07E-11	5.01E-04	1.95E-04
3.0000	3.72E-06	1.93E-02	1.39E-02
4.0000	9.77E-04	2.31E-01	2.03E-01
5.0000	2.70E-02	1.35E+00	1.41E+00
6.0000	2.40E-01	4.60E+00	6.02E+00
7.0000	1.12E+00	1.12E+01	1.85E+01
8.0000	3.49E+00	2.18E+01	4.46E+01
9.0000	8.30E+00	3.68E+01	9.08E+01
10.0000	1.64E+01	5.62E+01	1.62E+02

TABLE XII. Reaction rate for $^{40}\text{Ca}(\alpha, \gamma)^{44}\text{Ti}$ as a function of temperature. Listed are the rates calculated on the basis of measured resonances, and of the predicted resonances using the parameters given in table VI. For comparison also shown is the rate predicted with the statistical model code NON-SMOKER.

Temperature [GK]	$N_A < \sigma v >_{exp}$ [cm 3 s $^{-1}$ mole $^{-1}$]	$N_A < \sigma v >_{emp}$ [cm 3 s $^{-1}$ mole $^{-1}$]	$N_A < \sigma v >_{HF}$ [cm 3 s $^{-1}$ mole $^{-1}$]
.1000	0.00E+00	0.00E+00	1.63E-47
.1500	0.00E+00	1.96E-44	2.35E-38
.2000	0.00E+00	2.00E-35	9.41E-33
.3000	1.34E-39	1.65E-26	9.48E-26
.4000	2.95E-29	4.17E-22	2.39E-21
.5000	4.38E-23	1.70E-19	3.16E-18
.6000	5.43E-19	9.40E-18	7.43E-16
.7000	4.40E-16	5.90E-16	5.71E-14
.8000	6.51E-14	6.73E-14	2.01E-12
.9000	3.13E-12	3.18E-12	3.96E-11
1.0000	6.87E-11	6.97E-11	5.02E-10
1.5000	8.25E-07	8.29E-07	2.67E-06
2.0000	1.33E-04	1.37E-04	3.63E-04
3.0000	3.19E-02	3.86E-02	8.37E-02
4.0000	5.29E-01	7.47E-01	1.64E+00
5.0000	2.85E+00	4.49E+00	1.08E+01
6.0000	8.74E+00	1.47E+01	3.92E+01
7.0000	1.93E+01	3.39E+01	1.01E+02
8.0000	3.47E+01	6.27E+01	2.06E+02
9.0000	5.42E+01	9.97E+01	3.63E+02
10.0000	7.69E+01	1.43E+02	5.75E+02

REFERENCES

- [1] A. Chieffi, M. Limongi, O. Straniero *Astrophys.J.* **502**, 737 (1998)
- [2] D. Arnett *Ann.Rev.Astron.Astrophys.* **33**, 115 (1997)
- [3] F.-K. Thielemann *et al.* in *Proc. Summer School on "Nuclear and Particle Astrophysics"*, Aug. 1997, Guanajuato, Mexico; eds. J. Hirsch and D. Page, Cambridge Univ. Press (1998) p. 27
- [4] Hix W.R. & Thielemann F.-K. 1996, *Astrophys.J.*, 460, 869
- [5] Hix W.R. & Thielemann F.-K. 1999, *Astrophys.J.*, 511, 862
- [6] Hoffman R.D., Woosley S.E., Weaver T.A., Rauscher T., & Thielemann F.-K. 1999, *Astrophys.J.*, 521, 735
- [7] Freiburghaus C., Rembges J.-F., Rauscher T., Kolbe E., Thielemann F.-K., Kratz K.-L., & Pfeiffer B. 1999, *Astrophys.J.*, 516, 381
- [8] Van Wormer, L., et al. 1994 *Astrophys.J.*, 432, 326
- [9] Schatz H., Aprahamian A., Görres J., Wiescher M., Rauscher T., Rembges J.-F., Thielemann F.-K., Pfeiffer B., Möller P., Kratz K.-L., Herndl H., Brown B.A., & Rebel H. 1998, *Phys.Rep.*, 294, 167
- [10] E.K. Warburton, J. Wenner, in *Isospin in Nuclear Physics* ed. D.H. Wilkinson, North Holland Publ. (1969), p. 173
- [11] Arnould M. 1972, *Astr.&Astrophys.*, 19, 92
- [12] Thielemann F.-K., Arnould M. & Truran J.W. 1987, in *Advances in Nuclear Astrophysics*, ed. E. Vangioni-Flam (Gif sur Yvette: Editions Frontière), 525
- [13] Holmes J.A., Woosley S.E., Fowler W.A., & Zimmerman B.A. 1976, *At.Data Nucl. Data Tab.*, 18, 306
- [14] Woosley S.E., Fowler W.A., Holmes J.A., & Zimmerman B.A. 1978, *At.Data Nucl. Data Tab.* 22, 371
- [15] Cowan J.J., Thielemann F.-K. & Truran J.W. 1991, *Phys.Rep.* 208, 267
- [16] Hauser W. & Feshbach H. 1952, *Phys.Rev.*, 87, 366
- [17] Harney H.L., Weidenmüller H.A. & Richter A. 1977, *Phys.Rev. C*, 16, 1774
- [18] Tepel J.W., Hoffmann H.M. & Weidenmüller H.A. 1974, *Phys. Lett.*, 49B, 1
- [19] Rauscher T., Thielemann F.-K. & Kratz K.-L. 1997, *Phys.Rev. C*, 56, 1613
- [20] Rauscher T. & Thielemann F.-K. 1998, in *Stellar Evolution, Stellar Explosions, and Galactic Chemical Evolution*, ed. A. Mezzacappa (Bristol: IOP), 519
- [21] Jeukenne J.P., Lejeune A. & Mahaux C. 1977, *Phys.Rev. C*, 16, 80
- [22] Mahaux C. 1982, *Phys.Rev. C*, 82, 1848
- [23] McFadden L. & Satchler G.R. 1966, *Nucl.Phys.*, 84, 177
- [24] Fantoni S., Friman B.L. & Pandharipande V.R. 1981, *Phys.Rev.Lett.*, 48, 1089
- [25] Firestone R.B., Shirley V.S., Baglin C.M., Chu S.Y.F., & Zipkin J., *Table of Isotopes*, 8th edition (New York: Wiley)
- [26] Audi G. & Wapstra A.H. 1995, *Nucl.Phys.*, A595, 409
- [27] Blatt J.M. & Weisskopf V.F. 1952, *Theoretical Nuclear Physics* (New York: Wiley)
- [28] Myers W.D., Swiatecki W.J., Kodama T., El-Jaick L.J., & Hilf E.R. 1977, *Phys.Rev. C*, 15, 2032
- [29] Thielemann F.-K. & Arnould M. 1983, in *Proc. Int. Conf. on Nucl. Data for Science and Technology*, ed. K. Böckhoff (Dordrecht: Reidel), 762
- [30] Goriely S. 1998, *Phys.Lett.* B436, 10

- [31] Van Isacker P., Nagarajan M.A., & Warner D.D., 1992, *Phys.Rev. C*, 45, R13
- [32] Grimes S.M., Anderson J.D., Kerman A.K., and Wong C. 1972, *Phys.Rev. C*, 5, 85
- [33] Sargood D.G. 1982, *Phys.Rep* 93, 61
- [34] Harney H.L., Richter A. & Weidenmüller H.A. 1986, *Rev.Mod.Phys.*, 58, 607
- [35] Lane A.M. 1978, *Phys.Rev. C*, 18, 1525
- [36] Reiter J. & Harney H.L. 1990, *Z.Phys. A* 337, 121
- [37] Auerbach N., Hüfner J., Kerman A.K., and Shakin C.M. 1972, *Rev.Mod.Phys.*, 44, 48
- [38] Fuller G.M., Fowler W.A. & Newman M.J. 1982, *Astrophys.J.*, 252, 715
- [39] Coopermann, E.L., Shapiro, M.H. & Winkler, H. 1977, *Nucl.Phys.*, A284, 163
- [40] Jones G.A. 1987, The Properties of Nuclei, Second Edition (Oxford: Oxford University Press)
- [41] Schmalbrock P., Becker H.W. Buchmann L. Görres J. Kettner K.-U. Kieser W.E. Kräwinkel H. Rolfs C. Trautvetter H.-P. Hammer J.W. Azuma R.E. 1983, *Nucl.Phys.*, A398, 279
- [42] Maas et al. 1978, *Nucl.Phys.*, A301, 213
- [43] Cseh J., et al. 1982, *Nucl.Phys.*, A385, 43
- [44] Toevs J.W. 1971, *Nucl.Phys.*, A172, 589
- [45] Rogers D.W.O. Dixon W.R. Storey R.S. 1977, *Nucl.Phys.*, A281, 345
- [46] Erné, F.C. & van der Leun, C. 1964 *Nucl.Phys.* 52, 515
- [47] Clarke, R.E., Dunnam, F.E. & Van Rinsvelt, H.A. 1971 *Nucl.Phys.* A171, 298
- [48] Chakrabarty, D.R., Eswaran, M.A. & Ragoowansi, N.L. 1983 *Phys.Rev. C* 28, 1012
- [49] Endt P.M. 1990, *Nucl.Phys.*, A521, 1
- [50] Watson R.B. et al. 1973, *Nucl.Phys.*, A203, 209
- [51] Nahm C.W. & Thwaites T.T. 1967, *Nucl.Phys.*, A103, 503
- [52] Dixon W.R., Storey R.S. & Simpson J.J. 1977, *Phys.Rev. C*, 15, 1896
- [53] Dixon W.R., Storey R.S. & Simpson J.J. 1981, *Nucl.Phys.*, A363, 173
- [54] J. Görres, M. Wiescher, C. Rolfs 1989, *Astrophys.J.* **343**, 365
- [55] C. Iliadis *et al.* 1991, *Nucl.Phys.* **A533**, 153
- [56] C. Iliadis *et al.* 1993, *Nucl.Phys.* **A559**, 83
- [57] J.G. Ross *et al.* 1995, *Phys.Rev. C* **52**, 1681
- [58] C. Iliadis *et al.* 1994, *Nucl.Phys.* **A571**, 132
- [59] Lévai G. & Cseh J. 1988, *J. Phys. G Nucl. Phys.* 14, 467
- [60] U. Strohbusch *et al.* 1974, *Phys.Rev. C* **9**, 965
- [61] H.W. Fulbright *et al.* 1977, *Nucl.Phys.* **A284**, 329
- [62] H.J. Fisker, Master Thesis, University of Aarhus 1999

FIGURES

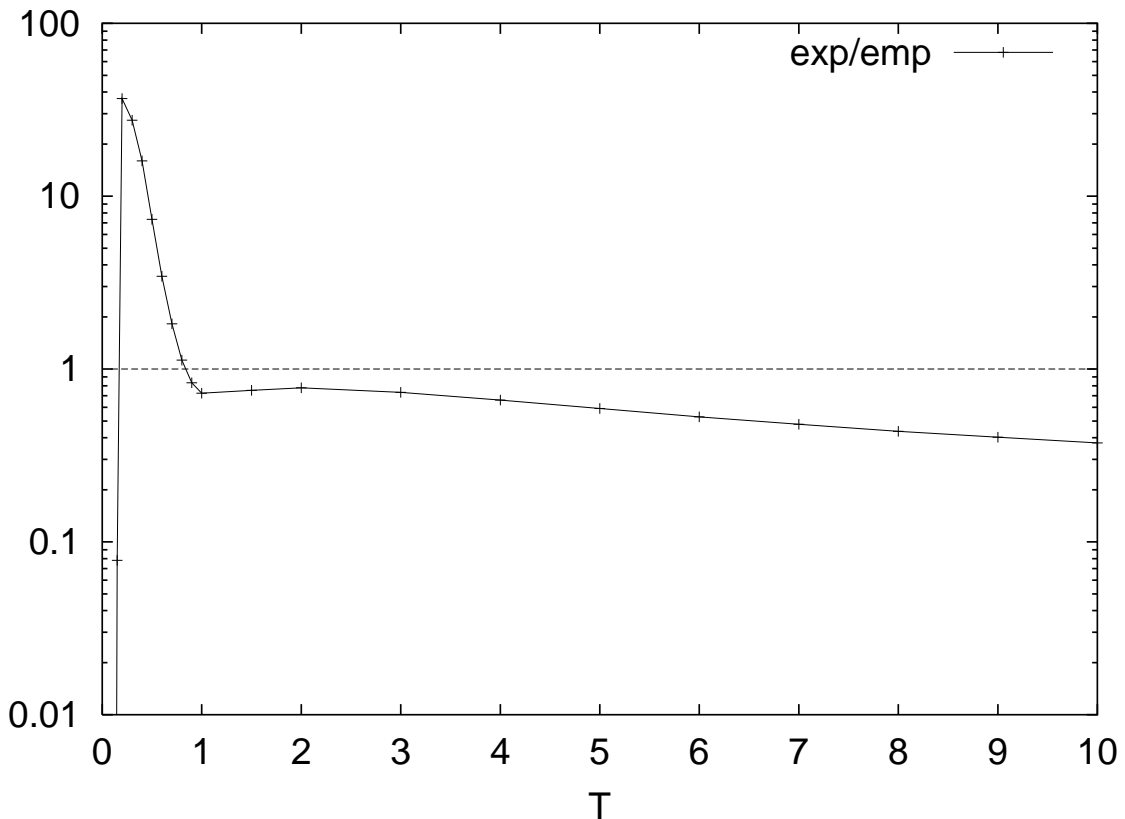


FIG. 1. Ratio of the 'experimental' rate (directly derived from α capture data) and the 'empirical' rate (derived from different sources; see text) for $^{20}\text{Ne}(\alpha, \gamma)$. The temperature T is given in GK.

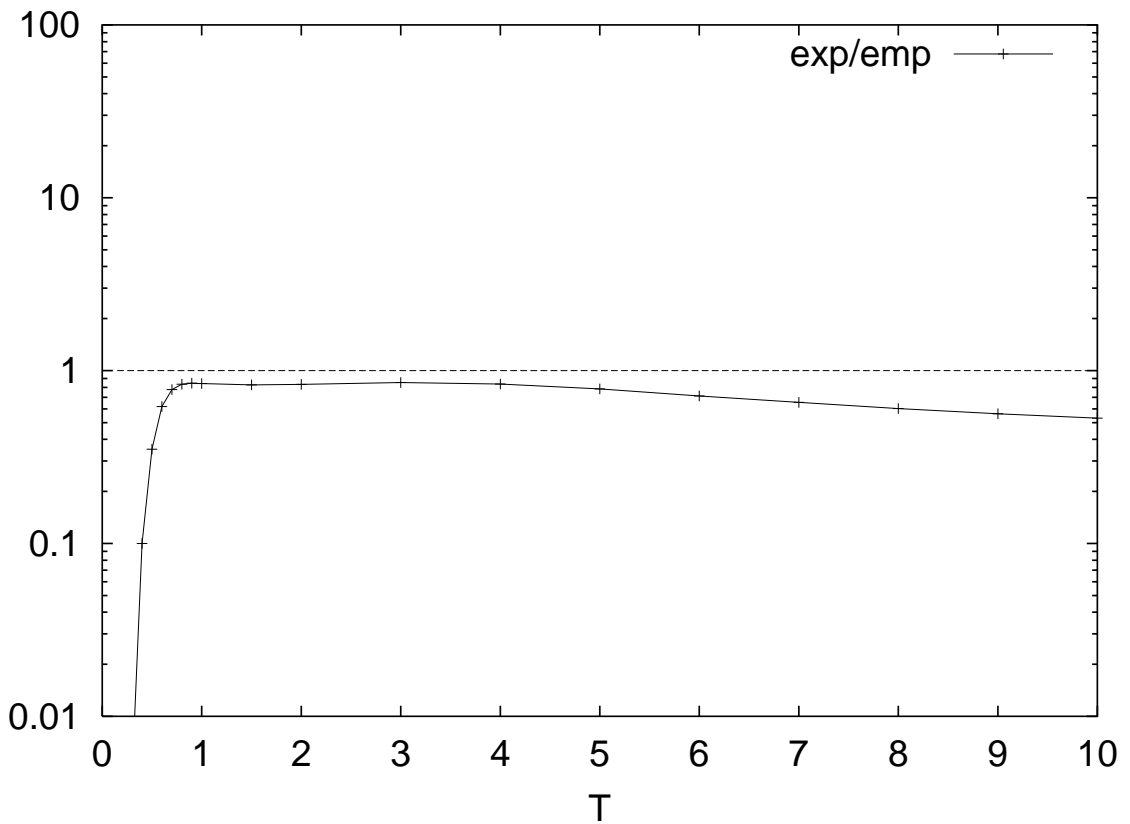


FIG. 2. Ratio of the 'experimental' rate (directly derived from α capture data) and the 'empirical' rate (derived from different sources; see text) for $^{24}\text{Mg}(\alpha, \gamma)$. The temperature T is given in GK.

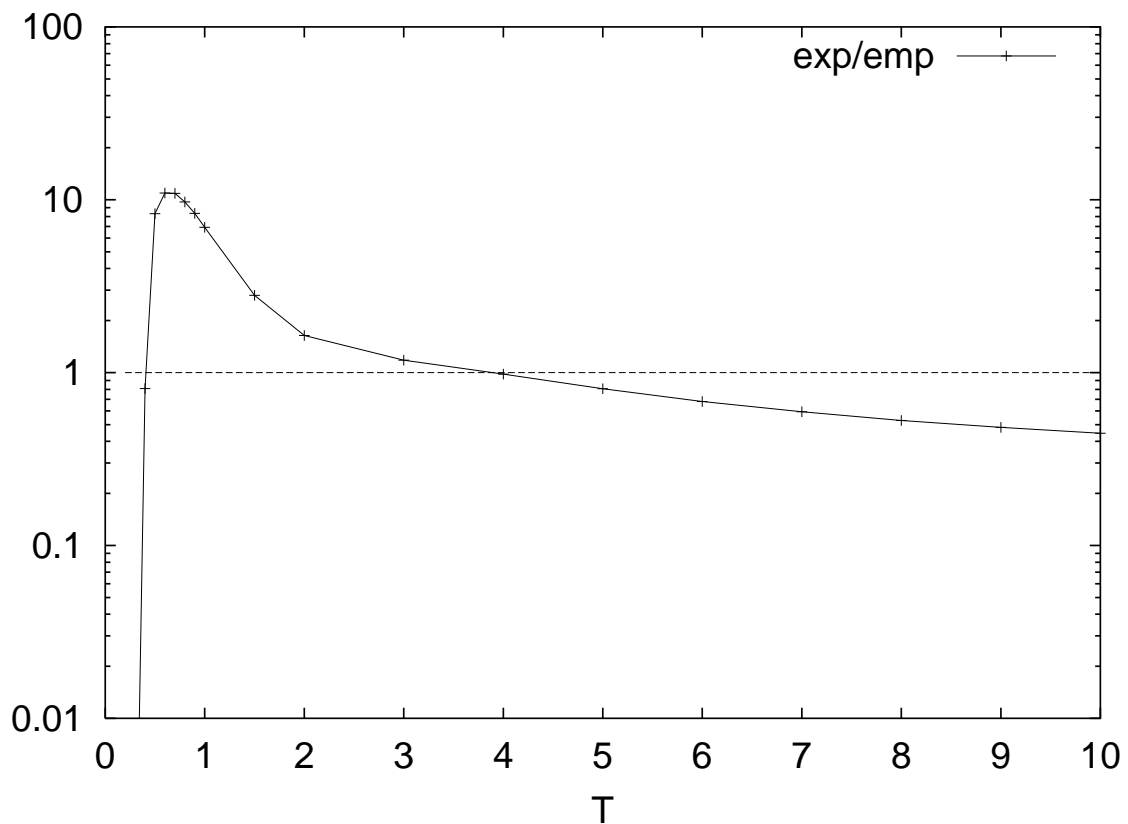


FIG. 3. Ratio of the 'experimental' rate (directly derived from α capture data) and the 'empirical' rate (derived from different sources; see text) for $^{28}\text{Si}(\alpha, \gamma)$. The temperature T is given in GK.

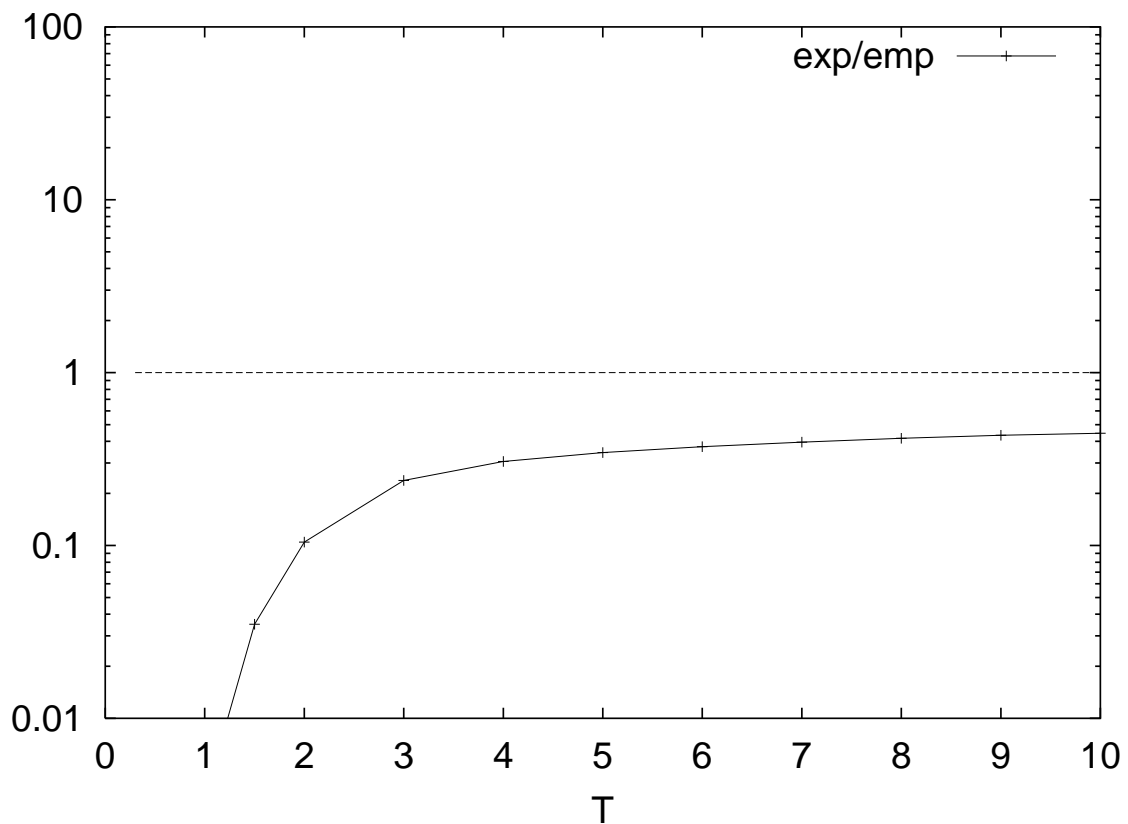


FIG. 4. Ratio of the 'experimental' rate (directly derived from α capture data) and the 'empirical' rate (derived from different sources; see text) for $^{32}\text{S}(\alpha, \gamma)$. The temperature T is given in GK.

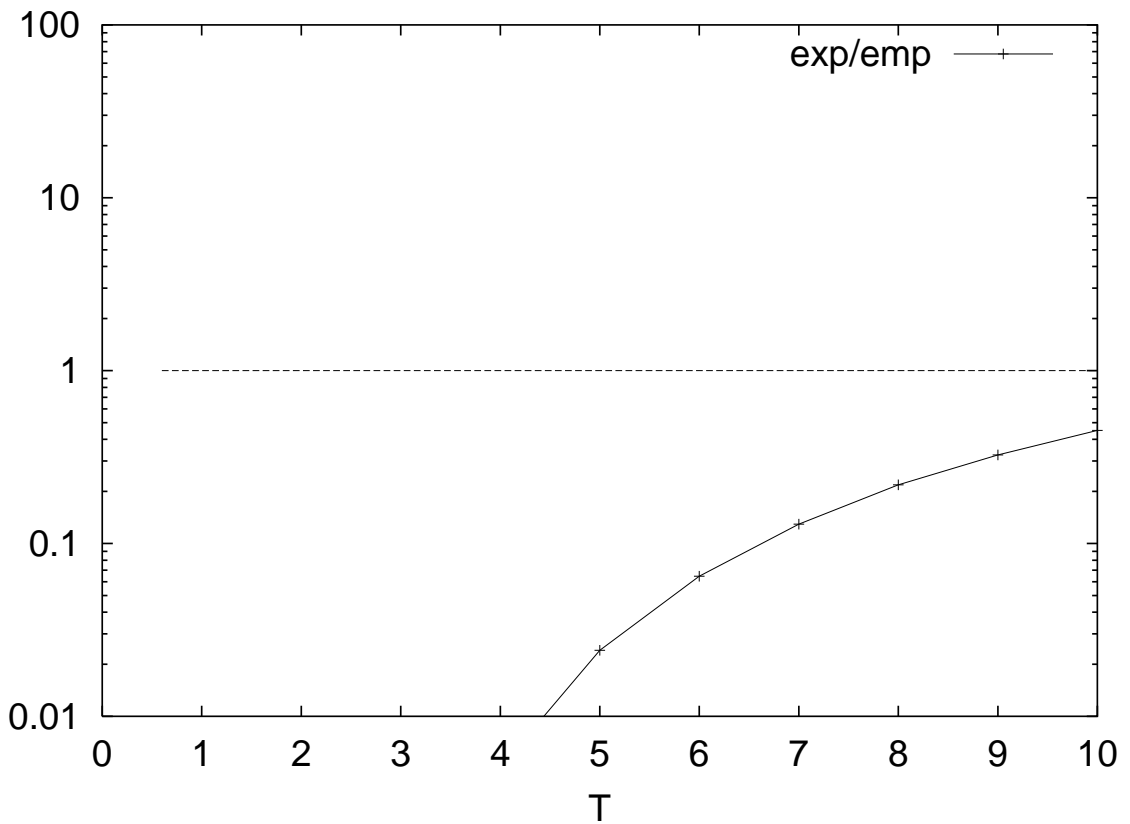


FIG. 5. Ratio of the 'experimental' rate (directly derived from α capture data) and the 'empirical' rate (derived from different sources; see text) for $^{36}\text{Ar}(\alpha, \gamma)$. The temperature T is given in GK.

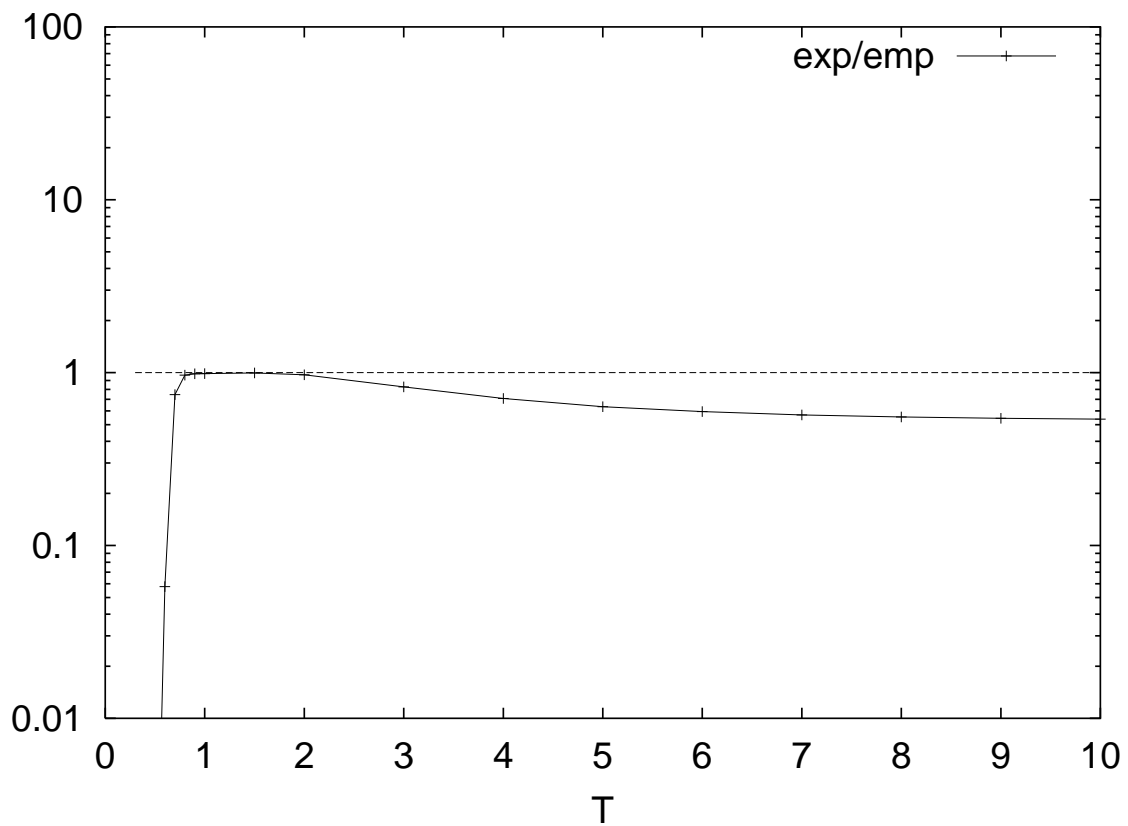


FIG. 6. Ratio of the 'experimental' rate (directly derived from α capture data) and the 'empirical' rate (derived from different sources; see text) for $^{40}\text{Ca}(\alpha, \gamma)$. The temperature T is given in GK.

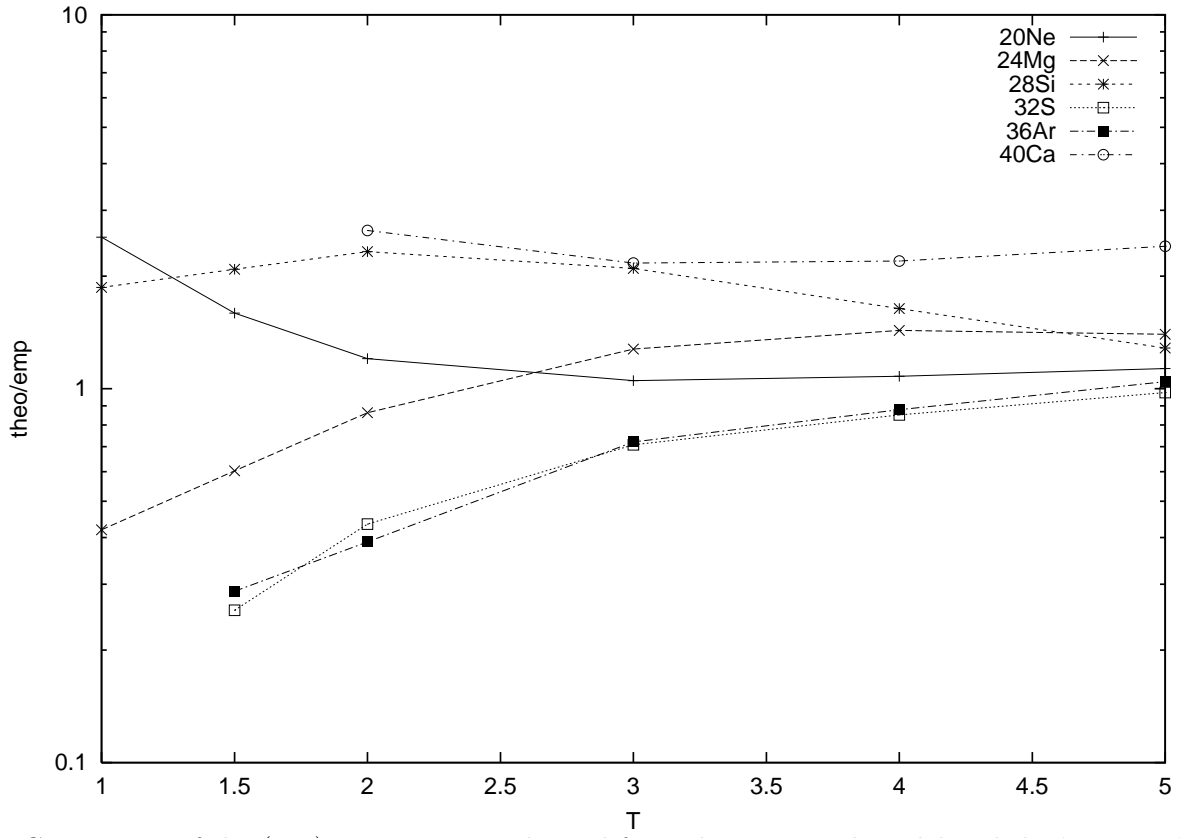


FIG. 7. Ratio of the (α, γ) reaction rates derived from the statistical model and the 'empirical' rates (see text) for the target nuclei ^{20}Ne , ^{24}Mg , ^{28}Si , ^{32}S , ^{36}Ar , and ^{40}Ca . The ratios are displayed within the astrophysically relevant temperature range. The temperature T is given in GK.